Chapter 3

Existence of exotic magnetic phases along with exchange bias and memory effect in frustrated beta-Mn Heusler alloy

3.1 Introduction

Heusler compounds, due to their exotic magnetic properties and wide range of applications in spintronics, are at the center of contemporary research. The quantum phenomenon that attracts current attention is spin-glass (SG) behavior, relaxation behavior, and magnetic memory effect (Binder & Young (1986); Jonason et al. (2000); Mydosh (1993)). The ternary formula of full Heusler compounds indicates that an appropriate choice of X, Y, and Z can make up a large group of possible Heusler compounds, e.g., Mn_2YZ, Fe_2YZ, Pt_2YZ, etc.(Graf et al. (2010); Wollmann et al. (2014) The Mn_2FeAl Heusler alloy,) which belongs to the large Mn_2YZ Heusler family,(Kroder et al. (2019)) is an exciting system to explore

due to its rich and complex magnetic phase diagram. However, crystallization disorder might lead to a partially disordered B_2 (Lv et al. (2020)) or $A2$ structure. Heusler alloys containing Mn and Fe transition elements are promising candidates for novel applications. Mn_2FeAl does not crystallize in the $L2_1$ structure, which most of the full Heusler alloys do. Interestingly, based on a theoretical electronic band structure study, it is predicted that Mn_2FeAl corresponds to an inverse x-type Heusler structure and belongs to half-metallic ferromagnets (Lv et al. (2020)). However, experimentally, it is found to be crystallized in the $\beta - Mn$ structure with a metallic nature (Ilyushin & Wallace (1976)). SG is a magnetic frustrated, disordered state caused by random spin freezing below a critical temperature. In SG, no long-range magnetic ordering is observed because it gets interrupted by the mixed interaction and frustrations, which originate due to competition between ferromagnetic (FM) and antiferromagnetic (AFM) interactions (Gardner et al. (2010)). SG was not significantly reported in Heusler alloys. The other phenomenon extensively studied by the experimentalist in Heusler alloys is exchange bias (EB) produced by interface magnetism. Co-based systems were of considerable interest for showing the well-established high Curie temperature and high spin polarization (Bainsla & Suresh (2016)). In the present study, we evaluate how the substitution of Co modifies the magnetic characteristics of Mn_2FeAl. For this purpose, we have studied all the equilibrium and non-equilibrium dynamics of $Mn_{1.5}Co_{0.5}FeAl$ (MCFA). The cluster glass state was confirmed, and it arose due to the freezing of large spin entities rather than the freezing of a single spin, which is responsible for the spin glass state. This compound belongs to the family of frustrated $\beta - Mn$ structures, as reported previously (Kroder et al. (2019)). Therefore, its glassy nature could arise due to its frustrated geometrical structure or competitive interactions. It also demonstrated all sorts of spin dynamics, such as magnetic relaxation, magnetic memory effect, and EB effect. However, there are few reports on the presence of EB in cubic alloys, which makes them very promising in the field of spintronic devices (Sharma

& Suresh (2015)). Some materials have incredibly high exchange bias value (Giri et al. (2021); Maniv et al. (2021)) and, thus, manifest enormous applications such as permanent magnets (Sort et al. (2001)), spin valves (Nakatani et al. (2012)), and applications based on spintronics properties (Anand et al. (2021); Sort et al. (2002)). In the present system, the obtained value of EB is larger than the parent system. So, along with the cluster glassy phase, the inclusion of the EB effect makes this system significant both from a basic and technological point of view.

3.2 Results and Discussions

The XRD pattern of the sample is shown in figure3.1. For the refinement, the initial values were estimated by (Gavrikov et al. (2019)) the crystal structure of MCFA crystallizes in the $\beta - Mn$ structure. In the $\beta - Mn$ structure, there are two inequivalent sites of Mn; one is at the 8c (Mn I) position and the other is at the 12d (Mn II) position. It was considered that the atoms on site were non-magnetic, whereas site II had a corner-sharing triangular structure. Due to this triangular arrangement of atoms, geometric frustration is present in the system. The powder XRD pattern of *MCFA* was refined with space group $P4_132$ (213). The parameters obtained from the refinement are listed in Table I. From the literature study, the suggested value of the lattice parameter is a = 6.3150 Å, and after Rietveld refinement, the obtained value of the lattice constant is comparable with the previously reported systems (Gavrikov et al. (2019); Hafner & Hobbs (2003)). For the magnetization study, figure3.2 shows the DC magnetization of MCFA at 20 Oe, using the zero-field-cooled warming (ZFCW) and field-cooled warming (FCW) procedures. It manifested the explicit glassy transition in ZFCW at 32.60 K; this peak corresponds to the freezing temperature (T_f). The $M(T)$ curve also exhibited the bifurcation between $ZFCW$ and FCW at the same temperature around 32.60 K, called irreversible temperature (T_{irr}), implying the nonergodicity in the $M(T)$ data. Other systems, such as Mn_2FeAl, $IrMnGa$,

and $Cr_{0.5}Fe_{0.5}Ga$ have shown T_f around 42, 30, and 22 K, respectively (Bag et al. (2018); Gavrikov et al. (2019); Kroder et al. (2019)), which is in close proximity with T_f obtained in this study. Systems with varying values of T_f depend on the concentrations of magnetic atoms present in the system (Yadav et al. (2019)).

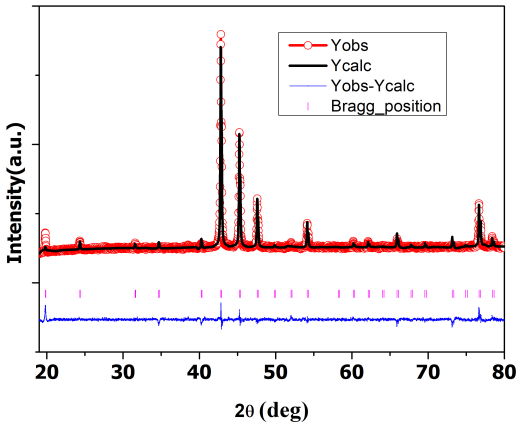

Fig. 3.1 Powder x-ray diffraction pattern of $Mn_{1.5}Co_{0.5}FeAl$ at room temperature (300 K)

Multiple ground states may cause frustration in the system, which leads to bifurcation. The uncoupling between $ZFCW$ and FCW is so prominent that it could not be extinguished over the application of a very high field, as shown in the dc susceptibility $(\chi_{dc} = M/H)$ curve in figure3.2(b). The bifurcation in the (χ_{dc}) curve is perhaps associated with the glassy phase[(Mydosh (1993)] or superparamagnetic (SPM) clusters[(Bedanta & Kleemann (2008)]. To throw some light on this behavior, we analyzed (χ_{dc}) *vs*. T for the higher order of magnetic fields. As the magnetic field was increased, the magnitude of (χ_{dc}) decreased, and the sharp kink converted into the plateau over a certain stretch of temperature in ZFC data. This is because as we increase the field, the anisotropic energy of the system and the corresponding energy associated with the applied external field are comparable, giving rise to the plateau region. Furthermore, a decrease in temperature creates an imbalance between the anisotropic energy and external field energy; hence, a bifurcation between $ZFCW$ and FCW was obtained. If bifurcation occurred due to non-interacting SPM clusters, the

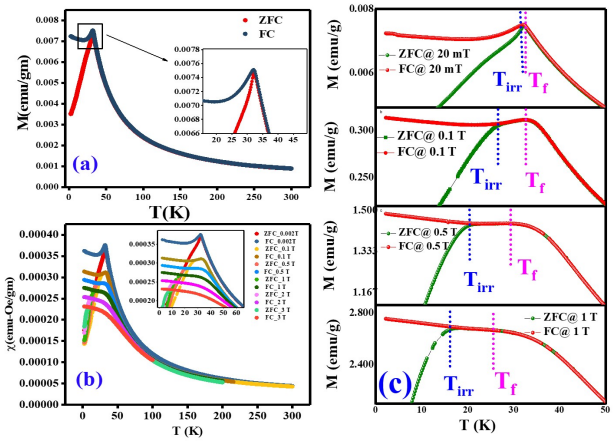

Fig. 3.2 . (a) dc magnetization of$Mn_{1.5}Co_{0.5}FeAl$ measured at 20 Oe in $ZFCW$ and FCW conditions. The inset provides a magnified view of the spin glass transition. (b) dc susceptibility (χ_{dc}) was measured at different fields in $ZFCW$ and FCW conditions. (c) dc magnetization was measured at different fields in $ZFCW$ and FCW conditions. The dash lines (blue for T_{irr} and pink for T_f are showing the shifting of T_{irr} and T_f

.

FCW curve of the $M(T)$ plot should have increased continuously below T_f, (Bedanta & Kleemann (2008)) but instead of this, the FCW the curve was decreased with a decrease in temperature. This indicates the presence of the SG phase in $MCFA$. Another exciting feature associated with the presence of glassy nature in the system is that T_{irr} and T_f tend to move toward the lower temperature side; however, the separation between them increases on increasing the magnetic field (Bag et al. (2018); Kumar et al. (2019)), shown in figure3.2 (c). Similarly, the divergence in χ_{dc} also decreases with the application of the magnetic field. These two characteristics made the clear presence of the spin glass state below T_f.

To get a deep insight into the presence of glassy nature in the system, isothermal magnetization $M(H)$ data are measured at regions below and above the transition temperature, as shown in figure3.3. The M(H) curve at 4 K showed a small hysteresis with unsaturated behavior up to ±6 T. Furthermore, $M(H)$ recorded from 25 to 300 K, as shown in figure3.3

is nonlinear at 25 and 50 K, which is due to the presence of dominating antiferromagnetic ordering in the system. As the temperature was increased further, magnetization varied linearly with the field, indicating entering the paramagnetic (PM) region with the presence of a small moment. The small hysteresis and nonlinear behavior with an unsaturated moment (up to ± 6 T) indicated the presence of weak ferromagnetic ordering along with a dominating antiferromagnetic ordering. However, at high temperatures, it showed a complete antiferromagnetic nature.

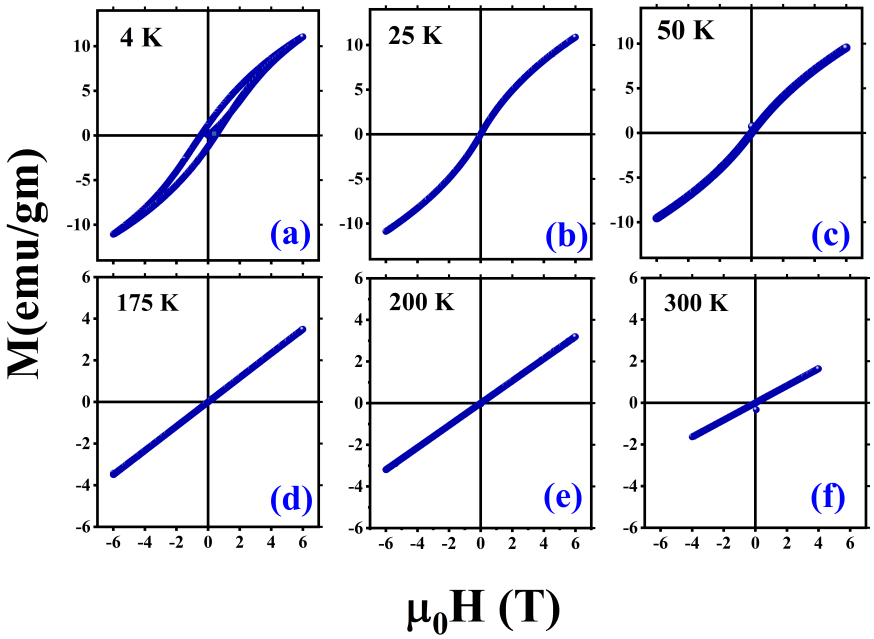

Fig. 3.3 Isothermal magnetization $M(H)$. Measured at 4 K (a), 25 K (b), 50 K (c), 175 K (d), 200 K (e), 300 K (f)

Another experimental technique for confirming SG in the frustrated system is ac susceptibility (χ_{ac}) (Cannella & Mydosh (1972); Kawamura & Taniguchi (2015)). In the 1970s, studies observed a very sharp cusp in ac susceptibility (Cannella & Mydosh (1972)). This sharp cusp is converted into a broader cusp after applying feeble ac fields (Kawamura & Taniguchi (2015)). Possible causes for the emergence of a sharp cusp in ZFC data as well as the bifurcation between ZFCW and FCW in the M-T curve, are

examined exclusively to deny the existence of SPM blocking. So, we have measured χ_{ac} vs T at different frequencies, as shown in figure 3.4 (a). The real part of ac susceptibility (χ') shows a peak around 32.60 K at 5 Hz frequency; this peak is positioned at the same temperature where the irreversibility between ZFC and FC curves occurred. So, apparently, according to spin dynamics, this peak corresponds to the glassy nature of MCFA. Figure 3.4 (a) illustrates that the peaks shift to the higher temperature side with an increased frequency from f = 5 Hz to f = 800 Hz. Another feature observed here was that below T_f χ' has a smaller magnitude for high frequencies, while above T_f, all the curves coincide. This behavior is also in accordance with the presence of spin glass in the system. The nature of glassy phases was distinguished with the help of the Mydosh parameter(K), which can be calculated as (Mydosh (1993))

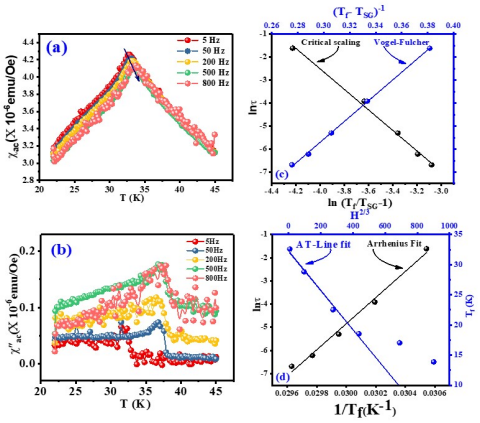

Fig. 3.4 Frequency-dependent ac susceptibility. (a) The real part of χ' measured at T_f shows the shifting with frequency. (b) The imaginary part of AC susceptibility shows steplike behavior. (c) and (d) showing the critical scaling fit, Vogel-Fulcher fit, Arrhenius fit, and linear behavior of T_f vs. $H^{\frac{2}{3}}$ shows the presence of the de Almeida-Thouless line

.

$$K = \frac{1}{T_f(\omega)} \frac{\Delta T_f(\omega)}{\Delta(\log_{10}\omega)} \tag{3.1}$$

The obtained value of K is 0.012, which typically lies in the range for cluster spin glass (CSG). Similar values of K are also observed for other systems such as Ga_2CoMn[(Samanta

et al. (2018)], $Cr_{0.5}Fe_{0.5}Ga$[(Bag et al. (2018)], $Mn_2Ni_{1.6}Sn_{0.4}$[(Ma et al. (2011)], and $Fe_{2-x}Mn_xCrAl$[(Yadav et al. (2019)], which lies in the CSG region. So, it rules out all the possibilities of the SPM state in the system. The value of K quantifies the interaction between the clusters and applied frequency. For instance, weakly interacting clusters would respond even at very low frequencies, while for strongly interacting clusters, a high frequency was required. Consequently, here the system has responded even at low frequencies. The imaginary part of ac susceptibility (χ'') possesses a step-like nature, shown in figure 3.4(b). This kind of behavior in (χ'') is shown in the SG regime and existed due to a frustrated ground state. All these features indicate the typical SG behavior of the system (Kundu et al. (2019)).

Three empirical models have been used to investigate the dependence of T_f on frequency in order to have some insight into the dynamics of spins:

- Critical-scaling law (Gunnarsson et al. (1988)): $(\tau = \tau_0 \exp\left(\frac{E_A}{K_B(T_f - T_{SG}}\right))$
- Vogel Fulcher law (Souletie & Tholence (1985)): $(\tau = \tau_0 \left(\frac{T_f}{T_{SG}} - 1\right)^{-z\nu})$
- Arrhenius law (Anand et al. (2021)): $(\tau = \tau_0 \exp\left(\frac{E_A}{K_B(T_f - T_{SG}}\right))$

Where τ is the relaxation time $\left(\tau = \frac{1}{2\pi f}\right)$, T_{SG} is the freezing temperature of spins, z is the dynamic critical exponent, and ν is the critical exponent of the correlation length. E_a corresponds to the activation energy and k_B is the Boltzmann constant. The critical scaling law is the basic law to analyze the dependence of frequency on shifting the peak temperature. For proper fitting, we reformulated the power law as

$$\log_{10}\tau = \log_{10}\tau_0 - z\nu \log_{10}\left(\frac{T_f}{T_{SG}} - 1\right) \tag{3.2}$$

Similarly, another empirical model is the VF model, which considers the interaction between the clusters. The parameters obtained after fitting, shown in figure 3.4 (c), from

both models mentioned above [(I), (II)] fall into the cluster spin glass category (Anand et al. (2021); Binder & Young (1986); Mydosh (1993)) and are summarized in Table II. The values of T_{SG} and E_a/k_B were almost comparable, suggesting the presence of finite interaction between the clusters. Now, to unravel the nature of the interaction between the clusters (Ruderman–Kittel–Kasuya–Yosida SG or short-range interaction type), (Tholence (1984)) used a criterion defined as

$$\delta T_{Th} = \frac{T_f - T_{SG}}{T_f} \tag{3.3}$$

After substituting the parameters (taking as T_{SG} = 30.11 K, T_f = 32.60 K), the obtained value δT_{Th} for our system is 0.076. This value indicates RKKY cluster spin glass interaction between the magnetic clusters (Samanta et al. (2018); Venkateswarlu et al. (2019)). Spin dynamics is not in good agreement with the Arrhenius model, as shown in figure 3.4 (d). The parameters obtained from Arrhenius fitting were not feasible. This law is only applicable where non-interacting or weakly interacting clusters were present, but its invalidity clarified the presence of interacting clusters in the spin glass region (Kroder et al. (2019); Souletie & Tholence (1985); Zhang et al. (2014)). The transition region that appeared in the $\chi_{(T)}$ curve was further examined in this section through the H-T phase space diagram (Höller & Read (2020)). The relation of T_{irr} with an external magnetic field (H) can be defined using equation 3.4

$$T_{irr}(H) = T_{irr}(0)(1 - AH^m) \tag{3.4}$$

In the H–T phase space diagram, two lines were observed: Gabay-Toulouse (GT) line ($m \sim 2$) (Gabay & Toulouse (1981)) and de Almeid–Thouless (AT) line ($m \sim 2/3$) (Chatterjee & Nigam (2002)). In the weak irreversible region, both AT and GT lines were observed, whereas in the strong irreversible region, only the AT line was observed.

Furthermore, in the H–T phase space the diagram shown in figure 3.4 (d), Tirr linearly varies with the $H_{dc}^2/3$ in the low field region is followed by the AT line. The AT line is usually followed by glassy systems, so the presence of bifurcation at T_{irr} corresponds to the cluster glassy phase.

The dynamics of spin glass are very slow and hard-relaxing, and it easily violates the equilibrium phase. Therefore, it manifests several fascinating non-equilibrium phenomena such as aging, memory, and rejuvenation effects (Jonason et al. (2000); Zhang et al. (2014)). To investigate the existence of nonergodicity in MCFA, the magnetic memory effect is measured in the ZFC and FC modes, as illustrated in figure 3.5 (a) and figure 3.5 (b), respectively.

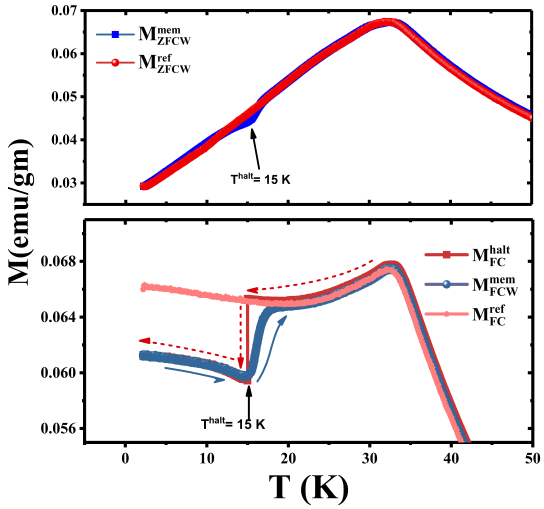

Fig. 3.5 Memory effect measured at 15 K. (a) ZFC and (b) FC curves

.

For the FC mode, we gradually cooled down the alloy in the presence of a 200 Oe magnetic field from a paramagnetic (PM) state to 2.2 K at 200 Oe. We put on hold the cooling process at T^{halt} = 15 K for a waiting time of t_w = 2 h. Before the waiting time began, the field was turned off, and the system was permitted to relax during the halted time. After the waiting time, the same field was applied, and the measurement was continued. The

magnetization measured in this procedure characterized a step-like behavior, represented as M_{FC}^{halt}. When the system was cooled up to 2.2 K, the measurement was again resumed from 2.2 to 50 K within the presence of the same magnetic field without any intervention during the warming cycle of the FC mode, represented as M_{FCW}^{mem}. Interestingly, during the FCW cycle, we have seen that M_{FCW}^{mem}. exhibits the same nature as in the FC cycle with an appearance of kink at a halt temperature. It is evident from the M_{FCW}^{mem}. curve that the system had claimed to recall its thermal magnetization history. A reference curve (M_{FC}^{ref}) with the same field without any intervention is also measured. Thus, it shows a clear presence of the memory effect in the MCFA alloy. Similarly, to check whether the memory effect is also present in the ZFC condition, isothermal magnetization vs temperature in the ZFC protocol was also measured. M_{ZFCW}^{mem} was measured during a warming procedure in the presence of the field. For validation, a traditional ZFC reference curve, M_{ZFCW}^{ref}, was measured without interruption. If the halted temperature region was excluded, these two curves would be found to coalesce with each other. As reported in Ref. 23, the existence of memory phenomena in ZFC data was attributed to the glassy nature of the alloy at low temperatures, and this was not found in systems that possess the SPM state. As a result of this, it reinforces the CSG behavior of the system. Furthermore, the magnetic relaxation behavior distinguishes various kinds of glassy systems, so the magnetization as a function of time (t) has been performed below T_f. In the past years, several researchers have studied magnetic relaxation below T_f in glassy systems, theoretically and experimentally (Chamberlin et al. (1984); Palmer et al. (1984)). A comprehensive model of glassy relaxation met three criteria: (i) It included the dynamics of spin, not merely statistics, (ii) the model used the interaction constraints, and last, (iii) it had also been using the hierarchy of the degree of freedom. It has progressively been evident that complicated, slowly relaxing, and strongly interacting systems frequently exhibit a stretched exponential behavior, equation:

This is known as the KWW(Kohlrausch–Williams–Watt) equation (Pal et al. (2019)), where Mo is the inherent magnetization, M_g is the glassy component of magnetization, τ is the characteristic time, and β is the stretching exponent. Which type of relaxation would be incorporated by the system was characterized by the obtained *beta* value. Usually, the value of *beta* lies between 0 and 1. In the above relation, if $\beta = 0$, the relation is modified into conventional Debye relaxation; therefore, this indicates that $M(t)$ is constant, which implies that there is no relaxation. The value of β directly comprises spin relaxation in addition to the nature of energy barriers present during relaxation. To analyze this, we have measured slow relaxation below freezing temperature. Therefore, the sample was cooled down from the PM region to 15 K under an applied field of 1000 Oe; after approaching 15 K, the field was turned off and the system was allowed to relax for 6000 s. Magnetization as a function of time (t) is depicted in figure 3.6. After fitting the data from the above relation, the obtained parameters are denoted as M_o= 0.08321 emu/gm, τ = 590 489 ± 6000, and β = 0.17. The value of β indicates the glassy nature of the system at 15 K with slow spin relaxation with time (Kleemann et al. (2010); Kroder et al. (2019); Kumar et al. (2019); Yadav et al. (2019)).

Usually, systems showing SG nature have widely been pursued to study the exchange bias (EB) effect (Karmakar et al. (2008); Kroder et al. (2019); Kumar et al. (2019); Kundu et al. (2019); Sahoo et al. (2019)). The presence of EB in any system can be encountered as a displacement of the hysteresis loop, either horizontally or vertically (Kumar et al. (2019)). Usually, the EB effect is detected at the FM/AFM (Anand et al. (2021)) interfaces; however, there have been several examples where the EB effect is found at some of the other interfaces such as CG/FM, FI/AFM, and AFM/CG (Pal et al. (2019)). A unidirectional EB is usually observed for SG systems. We have measured the M-H curve at 4 K in both ZFC and FC protocols, the FC loop is displaced on the field axis as shown in figure 3.7, and the ZFC loop does not show the EB effect. This shifting in FC is also consistent with the

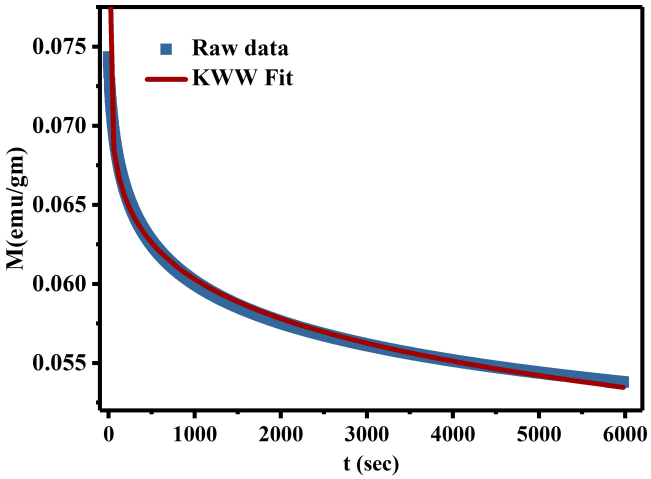

Fig. 3.6 Magnetic relaxation measured at 15 K under the application of 1000 Oe external field.

irreversibility found in M–T data in Fig. 2(a). When the alloy was cooled down from RT to 4 K in the zero field, all the spins froze together without any particular alignment. When the field was turned on, spins started to align with the applied field to conserve the energy of the system. However, due to frustration, a small value of magnetization was observed in comparison to FC, in which the field was already present before cooling, so the spins were bound to align in the direction of the field. However, the system still conserves its energy but with a larger value of magnetization. This was also analogous to the M–T data. Displacement observed in the M–H curve can be attributed to the EB or minor loop effect. To eliminate the possibility of the minor loop, an attempt was made to reduce the residual field and, then, the M–H curve in the FC mode at an applied field of 5 T was measured. The M–H loop is displaced in the negative field axis with an exchange bias of 478 Oe for a FC field of +5 T.

The EB value observed here was relatively higher than the other reported systems, such as in $Mn_{1.5}Fe_{1.5}Al$, the exchange bias field value was 99 Oe (Khorwal et al. (2022)). As depicted in $Mn_{50}Ni_{41-x}Sn_9Co_x$ ribbons, that exchange bias field is susceptible to Co

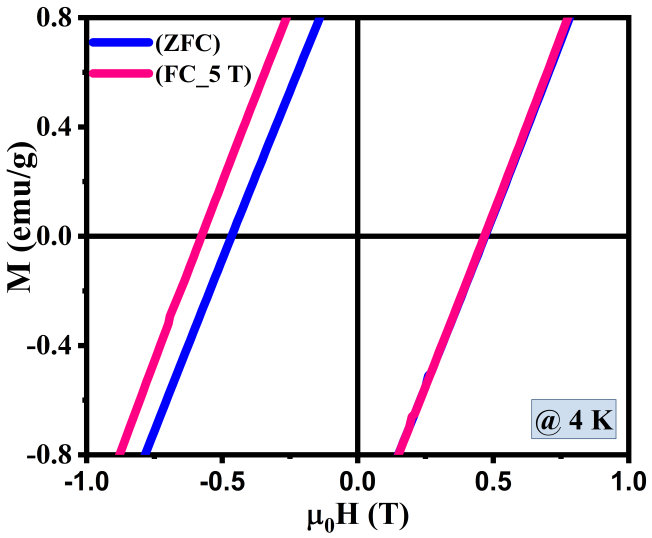

Fig. 3.7 Isothermal magnetization measures at 4 K in ZFC and FC conditions. The inset depicts the enlarged view of shifting along the positive X axis on the application of the +5 T field.

concentration (Zhai et al. (2014)). They observed a continuous tailoring of EB from 345 Oe to 3154 Oe. Therefore, the high value of EB in comparison to $Mn_{1.5}Fe_{1.5}Al$ was due to the presence of cobalt in MCFA. The intrinsic mechanism behind this was, as Khorwar et al. reported, that at low temperatures, the system showed a canonical spin glass state (Khorwal et al. (2022)). Similarly, in Mn_2FeAl, the value of the mydosh parameter is 0.02, again indicating the presence of a canonical spin glass state (Dash et al. (2020)). After the substitution of Co, it exhibits a cluster spin glass state. This is the main reason we get a high value of EB. The intrinsic mechanics behind the presence of exchange bias are usually attributed to exchange interactions at the interfaces between the pinning phase and the pinned phase. Here, the pinning phase is a cluster spin glass state. Zhao et al. also reported that the pinned phase remains unaltered while the pinning phase developed a shift from canonical to cluster spin glass as they increased the Co concentration (Zhao et al. (2014)).So due to the cluster spin glass state, we have seen a comparatively larger unidirectional anisotropy in MCFA, after cooling the sample in the presence of an external

magnetic field of 5 T. (Kroder et al. (2019)). studied half Heusler alloy IrMnGa and revealed the presence of the minor loop effect; unlike the present study, the EB effect was absent in their study. Therefore, the presence of the EB effect makes this system enormously fundamental and technologically relevant to scientific research.

3.3 Conclusions

We have investigated the magnetic properties of Co-substituted $Mn_{1.5}Fe_{1.5}Al$ alloy. The crystal structure of the system was confirmed to be β-Mn with space group $P4_132$. β-Mn structures are the frustrated structures due to two inequivalent sites of manganese (Mn). Therefore, dc magnetization presented the irreversibility between zero-field cooled warming (ZFCW) and field-cooled warming (FCW) curves at a temperature defined as Tirr. As a consequence, the spin glass phase was observed below $T_f \sim 33$ K (spin freezing temperature T_f). The spin-glass phase was confirmed by measuring the frequency-dependent AC susceptibility in the transition region. A broad cusp was observed near T_f. The shift in temperature with frequency was examined by three empirical models. The obtained parameters fall into the cluster's glass region. The unphysical values obtained from the Arrhenius model confirm the presence of interacting clusters in the cluster glass region. The type of interaction was confirmed by Tholence criteria, which ensures RKKY spin-glass interaction. Furthermore, the cluster glass phase was confirmed by observing the sluggish relaxation and memory effect in both protocols, ZFCW and FCW. The presence of a shifted hysteresis loop instead of a minor loop established the cluster spin glass of the system very well. The substantial value of exchange bias was observed in comparison with the parent compound Mn_2FeAl, due to Co doping in the studied system.